J Solid State Electrochem (2010) 14:101–107
DOI 10.1007/s10008-009-0795-4

ORIGINAL PAPER

AC impedance investigation of plating potentials on the catalytic activities of Pt nanocatalysts for methanol electrooxidation

Tao Huang · Rongrong Jiang · Deng Zhang · Jihua Zhuang · Wenbin Cai · Aishui Yu

Received: 19 November 2008 / Revised: 19 January 2009 / Accepted: 26 January 2009 / Published online: 11 February 2009

Abstract Pt nanocatalysts supported on glassy carbon (GC) were electrochemically deposited by cyclic voltammetry (CV) with different scanning potential ranges. The lower limit of potential was fixed at −0.25 V vs. saturated calomel electrode, whereas the upper limit of potential was adjusted to be 0.0, 0.20, 0.60, and 1.0 V. Scanning electron microscopy images showed that Pt microparticles are uniformly dispersed on the GC substrate and the agglomerated microparticles are composed of numerous nanoparticles. In addition, the catalytic capabilities of Pt/GCs for methanol electrooxidation were examined by CV, chronoamperometry, and electrochemical impedance spectroscopy in a solution of 0.5 M CH_3OH and 0.5 M H_2SO_4. The results demonstrate that the catalytic activities and stabilities of Pt catalysts prepared by the potential ranges from −0.25 to both 0.60 and 1.0 V for methanol electrooxidation were higher than the others, which may be due to their higher electrochemical active surface area, lower charge transfer resistance, and more preferred Pt crystallographic orientation.

Keywords Methanol oxidation · Pt nanoparticles · Electrocatalyst · Electrochemical impedance spectroscopy

Introduction

Direct methanol fuel cell (DMFC) is being widely investigated and considered as a prospective and potential power source for the application in transportation, portable electronics, residential power sources, etc., because of its high energy density, simple construction, easy operation, relative low operating temperature, and environmental benign [1–4]. The key component of a DMFC is the membrane electrode assembly (MEA), in which electrochemical reactions take place and electrical energy is produced. An MEA consists of three components: an anodic electrode, a cathode electrode, and a polymer electrolyte membrane. For electrochemical oxidation of methanol in acidic media, anode catalyst material most frequently consists of Pt particles. In recent years, a number of approaches have been reported for synthesis of Pt nanoparticles, such as microwave-assisted process [5–7], chemical reduction [8–10], and electrochemical deposition [11–13]. The electrochemical deposition method has some special advantages such as high purity of deposits and simple procedure of deposition. Many papers about Pt catalysts prepared by electrochemical deposition have been reported. Among them, the group of MME Duarte deposited different Pt particles on different carbon substrates using chronoamperometry by changing electrodeposition potential and time [14]. The dependence of morphology, microstructure, and electrochemical properties of platinum on different reduction potentials [11] and electrodeposition method such as fast square wave potential modulation [15] were also investigated. However, the effect of upper limit potential of cyclic voltammetry method on electrochemical-deposited platinum has not been reported so far.

This work aims to investigate the effect of plating potential ranges on the performance of Pt nanocatalysts for methanol electrooxidation. Our approach is to prepare Pt/glassy carbon (GC) by electrochemical cyclic voltammetry (CV) with different scanning potential ranges and the catalytic activity of Pt catalysts for methanol electrooxidation

T. Huang · R. Jiang · D. Zhang · J. Zhuang · W. Cai · A. Yu (✉)
Department of Chemistry,
Shanghai Key Laboratory of Molecular Catalysis and Innovative Materials, Institute of New Energy, Fudan University,
220 Handan Road,
Shanghai 200433, China
e-mail: asyu@fudan.edu.cn

in acid media were studied by CV, chronoamperometry (CA), and electrochemical impedance spectroscopy (EIS). It will provide a better insight into the selection of plating potential ranges for electrochemical deposition of Pt catalysts and the kinetics of methanol electrochemical oxidation in acidic media.

Experimental section

Preparation and characterization

The electrochemical experiments were carried out on an electrochemical workstation (CHI660A, CHI company) in a conventional three-electrode electrochemical cell using a platinum foil (12×12 mm) and a saturated calomel electrode (+0.241 V vs. normal hydrogen electrode) as the counter and reference electrodes, respectively. The glassy carbon electrode (φ 5 mm, geometric area is approximately 0.196 cm^2) sealed by poly(tetrafluoroethylene) was used as the working electrode for Pt deposition which was polished with 0.05-μm alumina powder, until a shiny mirror-like surface was obtained, and was then ultrasonicated for several minutes in deionized water. The GC electrode was further cleaned in 0.5 M H_2SO_4 by electrochemical CV with the potential range from −0.25 to 1.20 V at a scan rate of 0.05 V s^{-1}. Subsequently, the Pt catalysts supported on GC electrodes were prepared by CV in a solution of 2 mM potassium hexachloroplatinate (IV) and 0.5 M sulfuric acid with the scanning potential ranges of −0.25~0.0, −0.25~0.20, −0.25~0.60, and −0.25~1.0 V, at a scan rate of 0.05 V s^{-1} for 20 cycles. The catalysts were labeled as S1, S2, S3, and S4, respectively. The as-prepared Pt catalysts were characterized by scanning electron microscopy (SEM). SEM images were obtained on a Philips XL30 with an operating voltage of 20 kV.

Electrochemical measurement

The catalytic activities of the as-prepared catalysts for methanol oxidation were studied by means of CV and CA in a conventional three-electrode electrochemical cell as described above. The CV measurements were carried out in a solution of 0.5 M H_2SO_4 and 0.5 M CH_3OH at a scan rate of 0.05 V s^{-1}. To obtain chronoamperometry curves, the working electrode was polarized at 0.60 V in the same solution for 600 s. Electrochemical impedance measurements were conducted by sweeping the frequency from 100,000 to 0.005 Hz in a constant voltage mode at amplitude of 5 mV after polarizing at respective constant potential for 60 s. The electrode potential was set at 0.30, 0.40, 0.50, 0.55, 0.60, and 0.85 V.

Before each test, the solution was purged with N_2 for 15 min to remove O_2, and all electrochemical experiments were performed at room temperature. All the chemicals are analytical reagents and were used without any further purification.

Results

Electrochemical deposition of platinum

Figure 1 illustrates the cyclic voltammograms of GC in a solution of 2 mM K_2PtCl_6 and 0.5 M H_2SO_4 with different

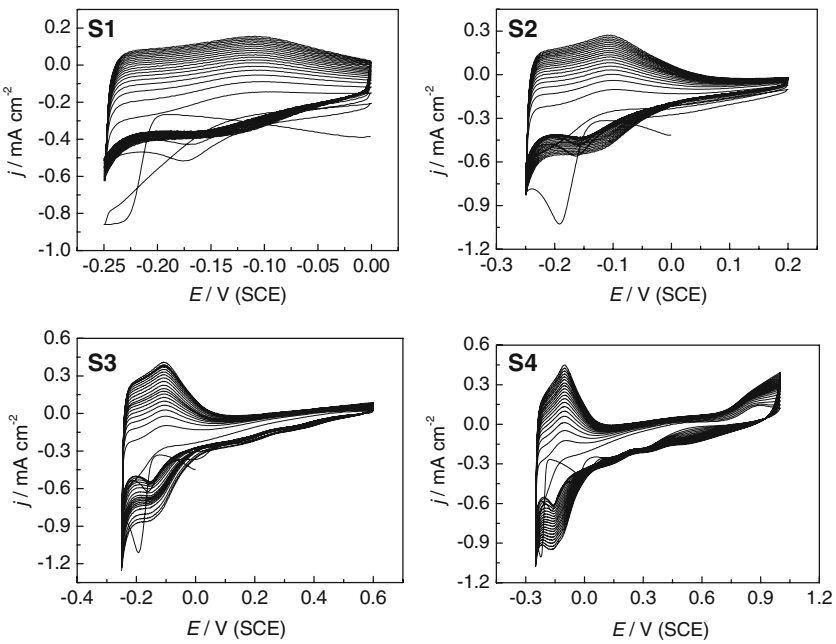

Fig. 1 Cyclic voltammograms for GC electrodes in the solution of 2 mM K_2PtCl_6 and 0.5 M H_2SO_4 with different scanning potential ranges, scan rate 0.05 V s^{-1}, cycling number is 20 cycles

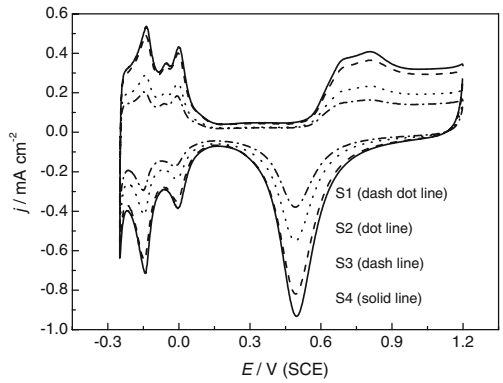

Fig. 2 Cyclic voltammograms of different Pt/GC electrodes in 0.5-M H_2SO_4 solution

scanning potential ranges at a scan rate of 0.05 V s^{-1} for 20 cycles. The onset potential of platinum deposition is around 0 V and there is a reduction peak at −0.16 V during negative-going potential scan, which can be attributed to the nucleation and diffusion-controlled growth of platinum particles [11, 16]. The onset potential of hydrogen evolution is at about −0.22 V. On the positive scan, a small peak can be seen at −0.10 V, which can be assigned to the desorption of hydrogen from platinum surface. The peak current densities (current/geometric area) increase with the increasing of cycling numbers, which means that the film is growing on the GC surfaces. After 20 cycles, the Pt/GC electrodes were removed from the solution and washed with deionized water.

Characterization

The as-prepared catalysts of Pt/GC were electrochemically characterized in 0.5 M H_2SO_4 solution at a scan rate of 0.05 V s^{-1}. Figure 2 displays the comparison of CV curves of S1, S2, S3, and S4. Well-defined CV features of a polycrystalline Pt electrode are observed on all Pt/GCs. In the potential range from −0.25 to 0.10 V, there are two pairs of redox peaks around −0.14 and 0.0 V, which are the hydrogen adsorption and desorption peaks. The redox peaks around −0.14 V is related to crystal face (110) site of Pt [17]. The number of adsorption sites on the faces (100), (111), and (110) of Pt are four, three, and five, respectively, in which, the face (110) is most favorable among these three basic crystal faces of Pt for methanol electrooxidation [18, 19]. The rank of current density (current/geometric area) of the current peak at −0.14 V is S4≈S3>S2>S1, which indicates that both catalysts S4 and S3 have much more crystal face (110) sites of Pt than any other two catalysts. This difference may be one of the important elements for different catalytic activity for methanol oxidation. The pair of current peaks at about 0.0 V is attributed to the well-known hydrogen adsorption/desorption, which is related to the crystal surface (111) site of Pt [17]. For S4 and S3, the redox peaks at 0.0 V are much stronger than S1 and S2, which means plating at relatively wide range generates much more Pt(111).

The electrochemical active surface area (EAS) of platinum catalyst was measured from the total electrical charge used in hydrogen desorption from cyclic voltammograms obtained in 0.5 M H_2SO_4 between −0.25 and 0.20 V, assuming that monolayer hydrogen atom coverage and the hydrogen desorption charge density of 210 μC cm^{-2} of smooth platinum surface [14, 20]. The electrical charge of hydrogen desorption (Q_H) measured by integration of the CV curves can be used to evaluate quantitatively the EAS of Pt/GCs by the well-known formula of EAS=Q_H/210. The calculated EAS of S1, S2, S3, and S4 are 1.15, 1.58, 2.00, and 2.14 cm^2, respectively. Clearly, the upper limit of scanning potential has significant effect on the active surface area of Pt catalysts. The active surface area of Pt catalyst increases basically with the increasing of the upper limit of scanning potential.

Figure 3 presents the typical SEM and transmission electron microscopy (TEM) images of the as-prepared Pt catalysts. These four Pt/GCs have similar morphology. It can be obviously seen from the SEM image that the spherical platinum microparticles were uniformly dispersed

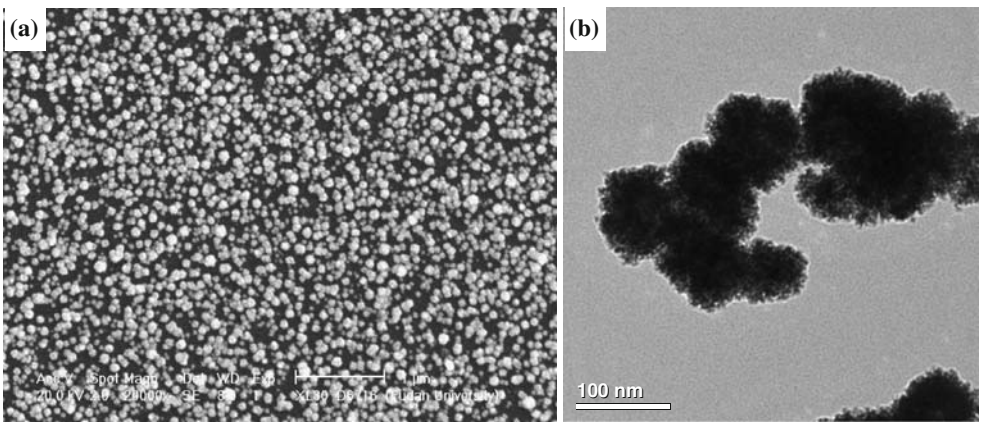

Fig. 3 Typical **a** SEM and **b** TEM images of as-deposited Pt particles

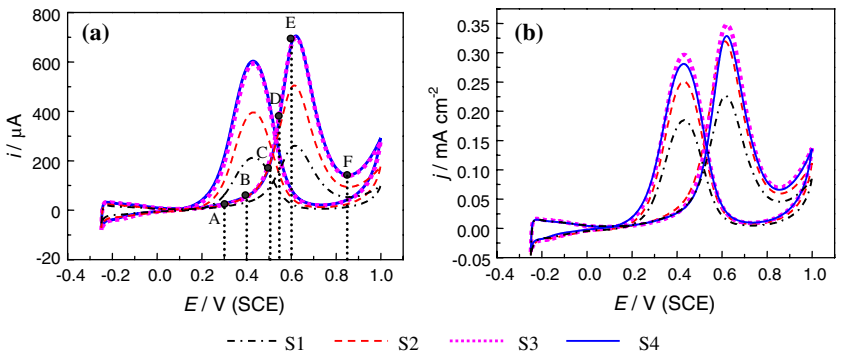

Fig. 4 **a**, **b** Cyclic voltammograms of Pt/GCs in a solution of 0.5 M CH_3OH and 0.5 M H_2SO_4

on GC substrate and the agglomerated microparticles are composed of numerous platinum nanoparticles (Fig. 3b).

Electrochemical properties for methanol oxidation

Figure 4 shows cyclic voltammograms of methanol electrooxidation on different Pt/GCs in a solution of 0.5 M CH_3OH and 0.5 M H_2SO_4 at a scan rate of 0.05 V s^{-1} expressed by current (Fig. 4a) and current density (current/EAS, Fig. 4b). It can be clearly seen that the onset potential for methanol oxidation on the four Pt/GCs are close, i.e., about 0.20 V. In the forward scan, methanol oxidation produced a symmetric anodic peak at 0.62 V for all of catalysts. In the reverse scan, there was also an anodic peak at 0.42 V, which is attributed to the reduction of the oxidized Pt oxide and the removal of the incompletely oxidized carbonaceous species formed in the forward scan [21–23]. So the ratio of the forward anodic peak current density (j_f) to the reverse anodic peak current density (j_b), j_f/j_b, could be used to describe the catalyst tolerance to carbonaceous species accumulation [24]. A low j_f/j_b ratio indicates poor oxidation of methanol to carbon dioxide during the anodic scan and excessive accumulation of carbonaceous residues on electrode surface. The ratios of j_f/j_b are 1.28, 1.22, 1.17, and 1.17, respectively. Obviously, four catalysts have close ratios of j_f/j_b, which illuminates that they have similar tolerance to carbonaceous species. However, from Fig. 4a, S3 and S4 have close current, which is higher than S1 and S2. From Fig. 4b, it can be seen that S3 and S4 still have higher current density, while S1 has the lowest one. Figure 5 presents the plots of current density vs. time for methanol electrooxidation at 0.60 V on different Pt/GC catalysts expressed by current (Fig. 5a) and current density (current/EAS, Fig. 5b). Obviously, S4 and S3 have higher initial and limiting both current and current densities than S1 and S2, which indicates better catalytic activities and stabilities for methanol oxidation. This result is well consistent with CV results in Fig. 4.

Electrochemical impedance spectroscopy of methanol oxidation

In order to further compare the activity of different Pt catalysts for methanol electrooxidation and to investigate kinetics and mechanism information, EIS measurements were carried out at different potentials, i.e., 0.30, 0.40, 0.50, 0.55, 0.60, and 0.85 V (points A, B, C, D, E, and F, respectively, in Fig. 4a). These potentials may represent different stages of methanol electrooxidation. From Fig. 5, it can be seen that the current changes sharply within the former 20 s. In order to record the impedance patterns at relatively stable current, EIS measurements were conducted by sweeping frequency from 100,000 to 0.005 Hz in a constant voltage mode at amplitude of 5 mV after polarizing at a respective potential for 60 s.

Figure 6 shows Nyquist plots of the impedance of methanol electrooxidation on different Pt catalysts at 0.30 V. A semicircle is evident in the complex-plane plots,

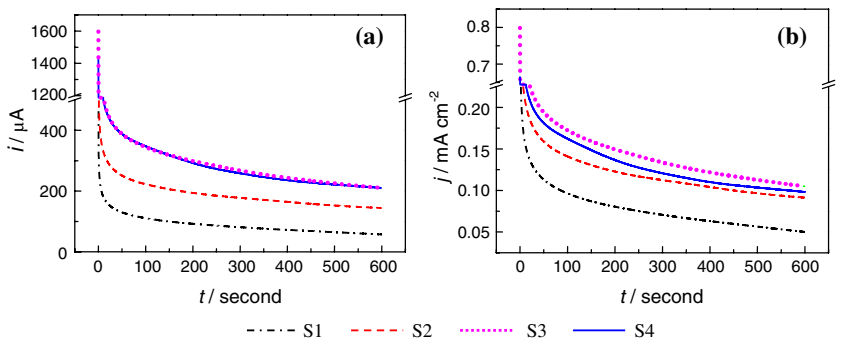

Fig. 5 **a**, **b** Chronoamperometry measurements of methanol oxidation in a solution of 0.5 M CH_3OH and 0.5 M H_2SO_4 on different Pt/GCs at 0.60 V

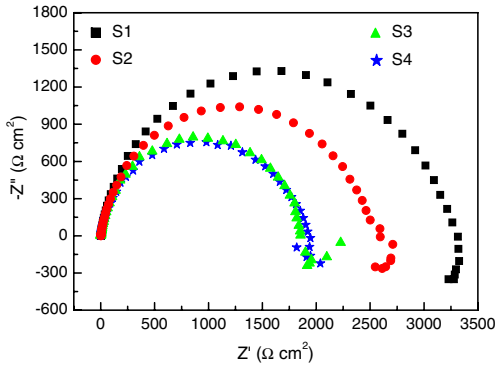

Fig. 6 Complex-plane impedance plots of Pt/GCs in a solution of 0.5 M CH_3OH and 0.5 M H_2SO_4 at 0.30 V

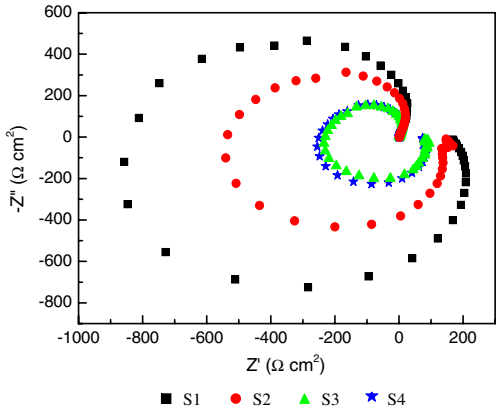

Fig. 8 Impedance patterns of methanol electrooxidation on the Pt/GCs in the solution of 0.5 M CH_3OH and 0.5 M H_2SO_4 at 0.50 V

which indicates the presence of resistive component and electrical double-layer capacitor. The rate-determining step is the methanol dehydrogenation. The solution resistance (R_s) is 5.47, 5.57, 5.54, and 5.42 Ω for S1, S2, S3, and S4, respectively. The charge transfer resistance (R_{ct}) is 8.47, 6.44, 4.72, and 4.87 kΩ for S1, S2, S3, and S4, respectively. The electrical double-layer capacitance (C) is respectively 68.0, 73.7, 83.0, and 97.5 μF for S1, S2, S3, and S4, which is calculated by $C=1/(R_{ct}\varpi^*)$. Obviously, the charge transfer resistance for S3 or S4 is nearly two times smaller than the other two. And the capacitance for S3 or S4 is larger than that of S1 or S2. So, it can be concluded that methanol dehydrogenation on Pt/GCs prepared by −0.25~0.60 or −0.25~1.0 V can be more easily carried out than that prepared by −0.25~0.0 and −0.25~0.20 V.

Figure 7 presents the impedance patterns of methanol electrooxidation on the Pt/GCs at 0.40 V. A semicircle at high frequency and pseudo-inductive behavior at low frequency (positive Z'' values) are observed. The transition from capacitive behavior to inductive behavior indicates that the rate-determining step may be changing. This pseudo-inductive behavior has been attributed to CO_{ads} oxidation [25]. It reveals from Fig. 7 that the rates of oxidation removal of the CO_{ads} by OH_{ads} are more rapid on S3 and S4 than on S2 and S1. Smaller charge transfer resistance for S3 or S4 may give higher faradic current, which is consistent with the CV results in Fig. 4.

In Figs. 8 and 9, the impedance plots wrap around the origin anti-clockwise and the capacitive arcs flip to the second quadrant with the real component of the impedance becoming negative, which is probably due to the passivation of electrode surface [26]. Due to the oxidation reaction of the intermediate of CO_{ads} which is the rate-determining step, the oxidation of CO_{ads} with OH_{ads} is very slow. The passivation can be explained by the formation of a large amount of CO_{ads} and OH_{ads} on the surface of Pt/GCs. The charge transfer resistance becoming negative may result from the passivation of the electrode surface, which is due to the reversible formation of oxide species [27]. Therefore, adsorption of methanol on Pt sites is inhibited due to an

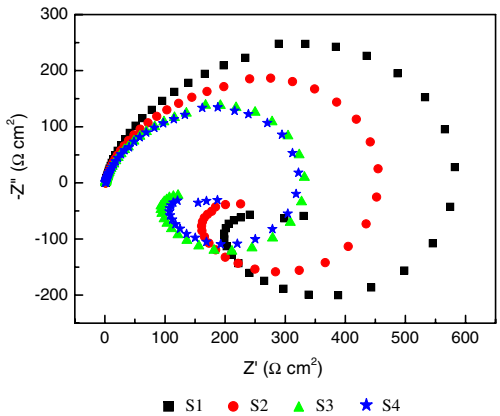

Fig. 7 Impedance patterns of methanol electrooxidation on the Pt/GCs in the solution of 0.5 M CH_3OH and 0.5 M H_2SO_4 at 0.40 V

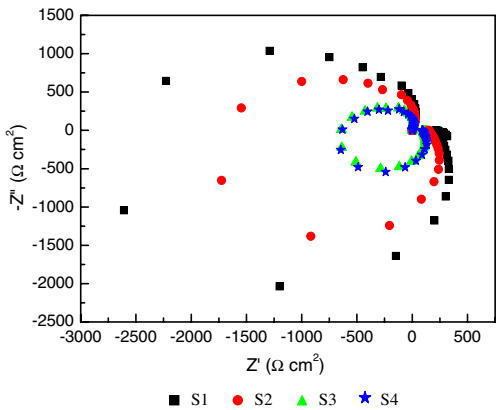

Fig. 9 Impedance patterns of methanol electrooxidation on the Pt/GCs in the solution of 0.5 M CH_3OH and 0.5 M H_2SO_4 at 0.55 V

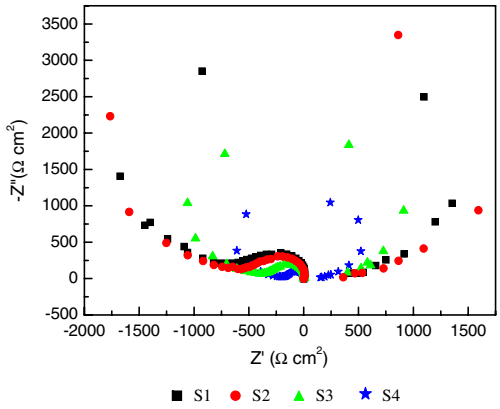

Fig. 10 Impedance patterns of methanol electrooxidation on the Pt/GCs in the solution of 0.5 M CH_3OH and 0.5 M H_2SO_4 at 0.60 V

increase of coverage of CO_{ads} and OH_{ads} on Pt sites and the electrooxidation rate has almost no obvious increase. Comparing the impedance plots in Figs. 8 and 9, it can be seen that the intensity of the passivation of catalyst surface for S3 and S4 is less than that of S1 and S2. These results demonstrate that the Pt catalysts prepared by the potential range of −0.25~0.60 and −0.25~1.0 V exhibit much higher activity compared with S1 and S2, which were respectively prepared by the potential range of −0.25~0.0 and −0.25~0.20 V.

The impedance patterns of methanol electrooxidation on the Pt/GCs in a solution of 0.5 M CH_3OH and 0.5 M H_2SO_4 at 0.60 V are presented in Fig. 10. The EIS behaviors of methanol oxidation have changed strongly for all Pt catalysts. Even so, S4 has smaller charge transfer resistance than the others.

Figure 11 shows the impedance patterns and equivalent circuit (insert) of methanol electrooxidation on the Pt/GCs in a solution of 0.5 M CH_3OH and 0.5 M H_2SO_4 at 0.85 V. At this high potential, oxygen evolution is considered the main reaction [28]. The solution resistance is about 5.5 Ω

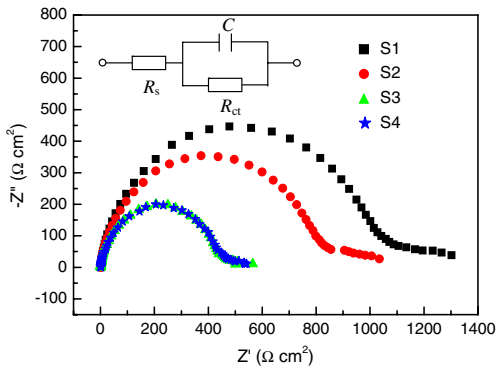

Fig. 11 Impedance patterns of methanol electrooxidation on the Pt/GCs in the solution of 0.5 M CH_3OH and 0.5 M H_2SO_4 at 0.85 V

for all Pt catalysts. The charge transfer resistance (R_{ct}) is 2,727, 2,168, 1,156, and 1,151 Ω for S1, S2, S3, and S4, respectively. The electrical double-layer capacitance (C) is 668, 841, 1,300, and 1,310 μF for S1, S2, S3, and S4, respectively. S3 and S4 have similar charge transfer resistances, which are about two times smaller than that of S1 and S2. And S3 and S4 also have close electrical double-layer capacitance, which is about two times larger than that of S1. So the EIS results demonstrate that S3 and S4 have similar catalytic activity, which is better than that of S1 and S2.

Discussion

Platinum catalysts with different electrochemical active surface areas were achieved by controlling different upper limits of scanning potentials. SEM images show that spherical platinum particles are well dispersed on GC substrate. The upper limits of scanning potentials do not have obvious effect on the platinum morphology; however, they have an important effect on the deposition of platinum including the process of nucleation, growth, dissolution, reduction, and oxidation. It can be seen from Fig. 1 that the onset potential for platinum deposition is around 0 V, so scanning potential higher than that could only lead to trace amount of platinum deposition and the total mass for sample S2, S3, and S4 should be very close to S1. Therefore, the better electrocatalytic properties of S3 and S4 for methanol oxidation can be ascribed to their larger electrochemical active surface areas, which can provide more active reaction sites of platinum for methanol oxidation and more preferred crystallographic orientation and thus improve their electrochemical reaction kinetics of methanol oxidation that were proven by EIS.

Conclusions

Four Pt/GC catalysts have been prepared by CV with different scanning potential ranges. The scanning potential ranges can affect the electrochemical active surface areas of Pt catalysts, which is one of the most important elements for the catalytic activity. The results of CV, CA, and EIS demonstrate that the scanning potential ranges have an important effect on the performance of Pt catalysts for methanol electrooxidation. The catalytic activities and stabilities of Pt catalysts prepared by the potential ranges from −0.25 V to both 0.60 and 1.0 V for methanol electrooxidation were higher than the others, due to their higher electrochemical active surface area, lower charge transfer resistance, and more preferred crystallographic orientation.

Acknowledgements This work is supported by a grant from the Key Program of Basic Research of the Shanghai Committee of Science and Technology, China (grant no. 08JC1402000).

References

1. Dyer CK (2002) J Power Sources 106:31. doi:10.1016/S0378-7753(01)01069-2
2. Dillon R, Srinivasan S, Aricò AS, Antonucci V (2004) J Power Sources 127:112. doi:10.1016/j.jpowsour.2003.09.032
3. Wasmus S, Kuver A (1999) J Electroanal Chem 461:14. doi:10.1016/S0022-0728(98)00197-1
4. Winter M, Brodd RJ (2004) Chem Rev 104:4245. doi:10.1021/cr020730k
5. Wang HW, Dong RX, Chang HY, Liu CL, Chen-Yang WC (2007) Mater Lett 61:830. doi:10.1016/j.matlet.2006.05.067
6. Chen WX, Lee JY, Liu ZL (2002) Chem Commun (Camb) 2588. doi:10.1039/b208600j
7. Zhao J, Chen WX, Zheng YF, Li X, Xu ZD (2006) J Mater Sci 41:5514. doi:10.1007/s10853-006-0276-4
8. Shim J, Joung KY, Ahn JH, Lee WM (2007) J Electrochem Soc 154:B165. doi:10.1149/1.2401032
9. Vanrheenen PR, Mckelvy MJ, Glaunsinger WS (1987) J Solid State Chem 67:151. doi:10.1016/0022-4596(87)90350-1
10. Koo IG, Lee MS, Shim JH, Ahn JH, Lee WM (2005) J Mater Chem 15:4125. doi:10.1039/b508420b
11. Whalen JJ, Weiland JD, Searson PC (2005) J Electrochem Soc 152:C738. doi:10.1149/1.2047407
12. Terzic S, Tripkovic D, Jovanovic VM, Tripkovic A, Kowal A (2007) J Serb Chem Soc 72:165. doi:10.2298/JSC0702165T
13. Rodrguez Nieto FJ, Pasquale MA, Cabrera CR, Arvia AJ (2006) Langmuir 22:10472. doi:10.1021/la0611716
14. Duarte MME, Pilla AS, Sieben JM, Mayer CE (2006) Electrochem Commun 8:159. doi:10.1016/j.elecom.2005.11.003
15. Custidiano E, Chialvo AC, Arvia AJ (1985) J Electroanal Chem 196:423. doi:10.1016/0022-0728(85)80038-3
16. Zubimendi JL, Vazquez L, Ocon P, Vara JM, Triaca WE, Salvarezza RC, Arvia AJ (1993) J Phys Chem 97:5095. doi:10.1021/j100121a041
17. Solla-Gullón J, Rodríguez P, Herrero E, Aldaz A, Feliu JM (2008) Phys Chem Chem Phys 10:1359. doi:10.1039/b709809j
18. Kinoshita K (1990) J Electrochem Soc 137:845. doi:10.1149/1.2086566
19. Stoyanova A, Naidenov V, Petrov K, Nikolov I, Vitanov T, Budevski E (1999) J Appl Electrochem 29:1197. doi:10.1023/A:1003482613323
20. Tran TD, Langer SH (1993) Anal Chem 65:1805. doi:10.1021/ac00061a027
21. Xu WL, Lu TH, Liu CP, Xing W (2005) J Phys Chem B 109:14325. doi:10.1021/jp051443y
22. Zhu J, Su Y, Cheng FJ, Chen J (2007) J Power Sources 166:331. doi:10.1016/j.jpowsour.2007.01.087
23. Manoharan R, Goodenough JB (1992) J Mater Chem 2:875. doi:10.1039/jm9920200875
24. Zhao GY, Xu CL, Guo DJ, Li H, Li HL (2006) J Power Sources 162:492. doi:10.1016/j.jpowsour.2006.06.082
25. Sugimoto W, Aoyama K, Kawaguchi T, Murakami Y, Takasu Y (2005) J Electroanal Chem 576:215. doi:10.1016/j.jelechem.2004.10.018
26. Wu G, Li L, Xu BQ (2004) Electrochim Acta 50:1. doi:10.1016/j.electacta.2004.07.006
27. Melnick RE, Palmore GTR (2001) J Phys Chem B 105:9449. doi:10.1021/jp003106p
28. Wang ZB, Yin GP, Shao YY, Yang BQ, Shi PF, Feng PX (2007) J Power Sources 165:9. doi:10.1016/j.jpowsour.2006.12.027